Ferromagnetism beyond Lieb's theorem

Natanael C. Costa,[1] Tiago Mendes-Santos,[1] Thereza Paiva,[1] Raimundo R. dos Santos,[1] and Richard T. Scalettar[2]

[1]*Instituto de Fisica, Universidade Federal do Rio de Janeiro Cx.P. 68.528, 21941-972 Rio de Janeiro RJ, Brazil*
[2]*Department of Physics, University of California, Davis, California 95616, USA*

The noninteracting electronic structures of tight-binding models on bipartite lattices with unequal numbers of sites in the two sublattices have a number of unique features, including the presence of spatially localized eigenstates and flat bands. When a *uniform* on-site Hubbard interaction U is turned on, Lieb proved rigorously that at half-filling ($\rho = 1$) the ground state has a nonzero spin. In this paper we consider a "CuO$_2$ lattice" (also known as "Lieb lattice," or as a decorated square lattice), in which "d orbitals" occupy the vertices of the squares, while "p orbitals" lie halfway between two d orbitals; both d and p orbitals can accommodate only up to two electrons. We use exact determinant quantum Monte Carlo (DQMC) simulations to quantify the nature of magnetic order through the behavior of correlation functions and sublattice magnetizations in the different orbitals as a function of U and temperature; we have also calculated the projected density of states, and the compressibility. We study both the homogeneous (H) case, $U_d = U_p$, originally considered by Lieb, and the inhomogeneous (IH) case, $U_d \neq U_p$. For the H case at half-filling, we found that the global magnetization rises sharply at weak coupling, and then stabilizes towards the strong-coupling (Heisenberg) value, as a result of the interplay between the ferromagnetism of like sites and the antiferromagnetism between unlike sites; we verified that the system is an insulator for all U. For the IH system at half-filling, we argue that the case $U_p \neq U_d$ falls under Lieb's theorem, provided they are positive definite, so we used DQMC to probe the cases $U_p = 0, U_d = U$ and $U_p = U, U_d = 0$. We found that the different environments of d and p sites lead to a ferromagnetic insulator when $U_d = 0$; by contrast, $U_p = 0$ leads to to a metal without any magnetic ordering. In addition, we have also established that at density $\rho = 1/3$, strong antiferromagnetic correlations set in, caused by the presence of one fermion on each d site.

I. INTRODUCTION

Within early mean-field theories (MFTs), the ground state of the single band Hubbard Hamiltonian [1], e.g., on a square lattice, was predicted to support both long range ferromagnetism (FM) and antiferromagnetism (AFM), with the two ordering wave vectors each occupying broad regions in the density (ρ)–interaction strength (U) phase space [2,3]. However, when treated with more accurate methods like quantum Monte Carlo (QMC) simulations and generalized Hartree-Fock approaches [4,5], this parity is broken. FM proves to be much more elusive [6,7], and indeed seems to be entirely absent from the square lattice phase diagram [8] except in "extreme" situations such as the Nagaoka regime of doping with a single electron away from half-filling at very large U (many times the kinetic energy bandwidth) [9,10]. The difficulty in achieving FM in the Hubbard Hamiltonian is unfortunate, since its explanation was one of the original motivations of the model [1,11].

How, then, might itinerant ferromagnetism be achieved in a model Hamiltonian? One route retains a single band but introduces frustration (e.g., through next-near-neighbor hopping) which shifts spectral weight to the band edges and minimizes the kinetic energy cost of the magnetic state [12–14]. Additional interaction terms such as next-neighbor direct exchange [1,15–17] or bond charge (correlated hopping) can also increase ferromagnetic tendencies, at least within MFT [18] or Gutzwiller approximation [19] treatments.

A second route to ferromagnetism is through the presence of several electronic bands. Within one picture, the resulting Hund's rule interactions play a crucial role [20,21]. A distinct scenario, and the one we carefully explore here, focuses instead on the presence of special noninteracting dispersion relations. In this context, a series of rigorous results were obtained. First, Lieb [22] established a theorem stating that in a class of bipartite geometries in any spatial dimension, with unequal numbers of sites $N_\mathcal{A}$ and $N_\mathcal{B}$ in the two sublattices ($\mathcal{A}$ and $\mathcal{B}$), the ground state has total spin $S = |N_\mathcal{A} - N_\mathcal{B}|/2$. The class of bipartite lattices for which the theorem was originally proved was subject to the following restrictions: the Hubbard repulsion U must be the same on every lattice site; hopping $t_{ij} c_i^\dagger c_j$ can only take place between sites ij in opposite sublattices; and there can be no single-particle chemical potential terms $\varepsilon_i c_i^\dagger c_i$. With these conditions, the Hamiltonian $\mathcal{H}$ is particle-hole symmetric (PHS), and each site, irrespective of being on the $\mathcal{A}$ or the $\mathcal{B}$ sublattice, is exactly half-filled. One should note, however, that Lieb himself warned that "spatial ordering is not implied" by a nonvanishing total spin; in addition, here the use of *ferromagnetism* should be understood as encompassing *unsaturated ferromagnetism*, though some authors (see the Erratum to Ref. [22]) advocate the use of *ferrimagnetism* in this case. A subsequent development was achieved [23] by establishing that spin-spin correlation functions $\langle \Phi_0 | \mathbf{S}_i \cdot \mathbf{S}_j | \Phi_0 \rangle$, where $|\Phi_0\rangle$ is the ground state, are positive (negative) for i and j on the same (different) sublattices; here, again, long range order is not necessarily implied [24,25].

Possible ferromagnetic order is closely tied to the fact that, in the noninteracting limit, tight-binding Hamiltonians on lattices with this geometry and obeying these conditions, have highly degenerate localized eigenstates, from which
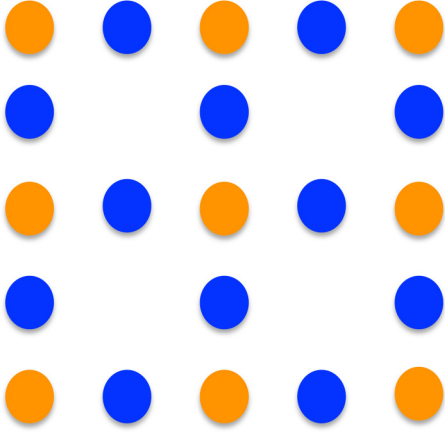
FIG. 1. The Lieb lattice (or CuO$_2$ lattice). The fourfold coordinated d sites appear in lighter color (orange) and belong to the $\mathcal{A}$ sublattice, while the twofold coordinated p sites appear in darker color (blue) and belong to the $\mathcal{B}$ sublattice.

linear combinations can be constructed to form a perfectly flat electronic band. At half-filling for the entire lattice, this flat band itself is precisely half-filled. Lieb's theorem was subsequently generalized to other graphs including the Kagomé and the square lattice with cross hoppings on half the squares [12]. It is notable that one of the essential ingredients in this route to ferromagnetism, PHS, is precisely what is broken in other scenarios such as the introduction of frustration. The implications of the Lieb theorem have also been explored for more general geometries [12,26], and one should note that flat-band ferromagnetism is independent of lattice dimensionality [27,28]. FM was found to occur away from the singular flat-band limit, i.e., in models with the perfect cosine dispersion characteristic of the Hubbard model with near-neighbor hopping only on linear, square, and cubic lattices [29].

One particular geometry to which Lieb's theorem applies is the CuO$_2$ lattice, also referred to as the Lieb lattice; see Fig. 1. In spite of the similarities with the actual CuO$_2$ sheets of high-T_c cuprates, one must stress that the relevant fillings for superconductivity in these materials is one hole per CuO$_2$ unit cell, rather than half-filling (three holes per unit cell), and in fact a significant site energy difference $\varepsilon_p - \varepsilon_d$ exists between occupation of the copper d and oxygen p orbitals (violating one of the restrictions of Lieb's theorem) [12]. Indeed, the cuprate materials exhibit AFM rather than FM.

Some consequences of the peculiar geometry of the Lieb lattice have been recently pursued in several theoretical studies [30–32]. While these studies did not include on-site interactions, which are directly linked with ferromagnetism, some effects of on-site repulsion U have only been investigated with the aid of dynamical mean-field (DMFT) [33,34]: it was found that each sublattice magnetization behaves monotonically with U, and this correlates with the local density of states. Finally, experimental realizations of the Lieb lattice as photonic lattices have been recently reported [35,36], and one should expect optical lattices could also be set up with this topology, motivated by the possibility of engineering ferromagnetic states through the control of interactions.

In view of this, several issues regarding the existence of ferromagnetism on the Lieb lattice should be addressed, and here we use determinant quantum Monte Carlo (DQMC) which treats the interacting electron problem exactly on lattices of finite size. First, a detailed analysis of the sublattice-resolved spatial decay of spin correlations and order parameters would add considerably to the understanding of how the basic units conspire to yield a robust polarized state. Second, can ferromagnetism still be found if one deviates from the conditions of Lieb's theorem, e.g., by relaxing the constraint of uniform U, i.e., allowing for $U_d \neq U_p$ (on "oxygen" and "copper" sites, respectively)? We then go beyond Lieb's theorem by distinguishing two situations, namely, the case where both U_p and U_d are nonzero, and the cases in which the on-site repulsion is switched off on either p sites or d sites. Away from half-filling, DQMC simulations are plagued by the infamous "minus-sign problem," which prevents us from reaching very low temperatures. Nonetheless, we can still shed some light into the effects on magnetic ordering by switching off the repulsion on either p or d sites.

The paper is organized as follows. In Sec. II we present the main features of the Hubbard Hamiltonian on the Lieb lattice, and highlight the DQMC method together with the quantities of interest. The results for the homogeneous and inhomogeneous lattices at half-filling are presented in Secs. III and IV, respectively; the behavior away from half-filling is briefly analyzed in Sec. V. Our main conclusions are then summarized in Sec. VI.

II. THREE-BAND HUBBARD HAMILTONIAN AND QUANTUM MONTE CARLO METHODOLOGY

The particle-hole symmetric three-band Hubbard Hamiltonian on a Lieb lattice,

$$
\begin{aligned}
\hat{H} - \mu \hat{N} = &-t_{pd} \sum_{\mathbf{r}\sigma} \left(d_{\mathbf{r}\sigma}^{\dagger} p_{\mathbf{r}\sigma}^{x} + d_{\mathbf{r}\sigma}^{\dagger} p_{\mathbf{r}\sigma}^{y} + \text{H.c.} \right) \\
&- t_{pd} \sum_{\mathbf{r}\sigma} \left(d_{\mathbf{r}\sigma}^{\dagger} p_{\mathbf{r}-\hat{x}\sigma}^{x} + d_{\mathbf{r}\sigma}^{\dagger} p_{\mathbf{r}-\hat{y}\sigma}^{y} + \text{H.c.} \right) \\
&+ \sum_{\mathbf{r}\alpha} U_{\alpha} \left(n_{\mathbf{r}\uparrow}^{\alpha} - \frac{1}{2} \right) \left(n_{\mathbf{r}\downarrow}^{\alpha} - \frac{1}{2} \right) \\
&+ \sum_{\mathbf{r}\alpha\sigma} \varepsilon_{\alpha} n_{\mathbf{r}\sigma}^{\alpha} - \mu \sum_{\mathbf{r}\alpha\sigma} n_{\mathbf{r}\sigma}^{\alpha} \quad (1)
\end{aligned}
$$

contains inter- and intracell hopping t_{pd} between a (copper) d and two (oxygen) p^x, p^y orbitals. In this paper we consider the on-site repulsion both as homogeneous, $U_p = U_d = U$, in accordance with Lieb's theorem, but also inhomogeneous, with either $U_p = 0$, $U_d \neq 0$ or $U_p \neq 0$, $U_d = 0$. In all cases, we set the local orbital energies $\varepsilon_p = \varepsilon_d = 0$ and global chemical potential $\mu = 0$. With these choices, particle-hole symmetry holds even in the inhomogeneous case, which yields half-filling $\rho = 1$.

For a model in which all sites $\mathbf{r}$ and orbitals α have the same on-site U, the two ways of writing the interaction $U n_{\mathbf{r}\uparrow}^{\alpha} n_{\mathbf{r}\downarrow}^{\alpha}$ and $U(n_{\mathbf{r}\uparrow}^{\alpha} - \frac{1}{2})(n_{\mathbf{r}\downarrow}^{\alpha} - \frac{1}{2})$ differ only by a shift in the choice of the zero of *global* chemical potential, so the physics is completely identical. However, if U_{α} depends on α (or $\mathbf{r}$), then changing to a particle-hole symmetric form corresponds

to an *orbital dependent* shift, i.e., an unequal change in the individual ε_α. The symmetric form corresponds to a special choice in which the occupancies of all orbitals are identically half-filled. Typically this choice is not obeyed in a real material, where each orbital has a unique filling. However, since it is a prerequisite for the applicability of Lieb's theorem, we impose it here.

The magnetic behavior is characterized by the local moments

$$\langle m_\alpha^2 \rangle = \langle (n_{\mathbf{r}\uparrow}^\alpha - n_{\mathbf{r}\downarrow}^\alpha)^2 \rangle \tag{2}$$

and also by the real space spin-spin correlation functions

$$c^{\alpha\beta}(\mathbf{r}) = \langle c_{\mathbf{r_0}+\mathbf{r}\downarrow}^{\alpha\dagger} c_{\mathbf{r_0}+\mathbf{r}\uparrow}^{\alpha} c_{\mathbf{r_0}\uparrow}^{\beta\dagger} c_{\mathbf{r_0}\downarrow}^{\beta} \rangle, \tag{3}$$

which measure the result of raising a spin on site $\mathbf{r_0}$ in orbital β and its subsequent lowering at site $\mathbf{r_0} + \mathbf{r}$ in orbital α. The Fourier transforms of $c^{\alpha\beta}(\mathbf{r})$ are the magnetic structure factors,

$$S^{\alpha\beta}(\mathbf{q}) = \sum_{\mathbf{r}} c^{\alpha\beta}(\mathbf{r}) e^{i\mathbf{q}\cdot\mathbf{r}}. \tag{4}$$

In the ferrimagnetic state proposed by Lieb, $c^{\alpha\beta}(\mathbf{r}) > 0$, when α and β are both d, or both p orbitals, while for unlike orbitals $c^{\alpha\beta}(\mathbf{r}) < 0$. We will focus on FM, $\mathbf{q} = 0$.

In order to probe the metallic or insulating character of the system, a useful quantity is the electronic compressibility, defined as

$$\kappa = -\frac{1}{\rho^2} \frac{\partial\rho}{\partial\mu}, \tag{5}$$

where ρ is the electronic density. The properties of the Hamiltonian Eq. (1) will be solved using determinant quantum Monte Carlo (DQMC) [7,37,38]. This method provides an exact solution, on real-space lattices of finite size, subject to statistical error bars and (small) "Trotter errors" from the discretization $\Delta\tau$ of imaginary time (inverse temperature). We have chosen $\Delta\tau$ small enough so that these Trotter errors are comparable to, or less than, the statistical errors on $c^{\alpha\beta}(\mathbf{r})$ and $S^{\alpha\beta}(\mathbf{q})$. We define the lattice spacing ($a = 1$) as the distance between nearest d sites; accordingly, the finite size L (in units of lattice spacing) is given by the number of d sites along one direction, while the numerical effort is actually measured by the number of lattice sites, $N_s \equiv 3(L \times L)$. Lattice separations along the horizontal or vertical directions with $|\mathbf{r}|$ integer correspond to correlations between like orbitals, whereas half-integral $|\mathbf{r}|$ denote unlike orbitals.

III. THE HOMOGENEOUS LATTICE

Figure 2 shows the temperature evolution of the local moment on d and p sites. Both moments start at the common high temperature value $\langle m_\alpha^2 \rangle = \frac{1}{2}$ and become better formed as the temperature crosses the energy scale $T \sim U$. At low temperatures, the moments stabilize in plateaux with $\langle m_\alpha^2 \rangle < 1$, which reflect residual quantum fluctuations arising from $t_{pd}/U \neq 0$. These fluctuations are larger for the d sites, which have four neighboring p sites, than for the p sites which have only two neighboring d sites. It is also interesting to note that the local moment for the usual square lattice $\langle m_{\text{square}}^2 \rangle$ is such that $\langle m_d^2 \rangle < \langle m_{\text{square}}^2 \rangle < \langle m_{p^{x(y)}}^2 \rangle$.
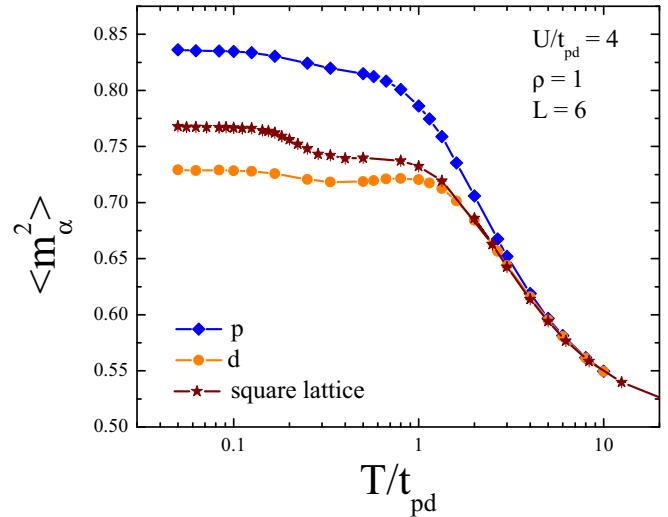

FIG. 2. Temperature evolution of the local moment on d and p sites of the Lieb lattice (linear-log scale). The fourfold coordinated d sites have a lower moment than the twofold coordinated p sites. Moment formation occurs mainly when $T/t_{pd} \sim U$, but a smaller signal is also seen at $T/t_{pd} \sim J$, the exchange energy. Here, and in all subsequent figures, when not shown, error bars are smaller than symbol size.

Intersite spin correlations develop at lower temperatures associated with the exchange energy scale $J \sim t_{pd}^2/U$. Figure 3 illustrates the different behaviors of correlations with the distance (all consistent with the rigorous results for their signs, as derived in Ref. [23]), at a fixed low temperature
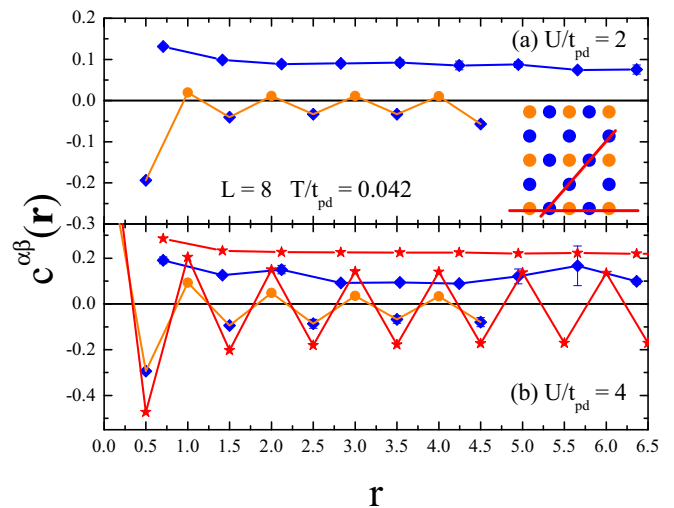

FIG. 3. Spatial dependence of spin-spin correlation functions, Eq. (3), at a fixed temperature, for $U/t_{pd} = 2$ (top panel) and $U/t_{pd} = 4$ (bottom panel). In each panel, diamonds and circles, respectively, represent positions of p and d sites, while stars on the bottom panel are data for the Heisenberg model. Curves going solely through diamonds (blue curves) correspond to placing the origin at a p site, and $\mathbf{r}$ running over p sites along a straight line at an angle of $45°$ (see the inset); curves alternating between diamonds and circles correspond to placing the origin on a d site, and $\mathbf{r}$ running along a horizontal line (see the inset).
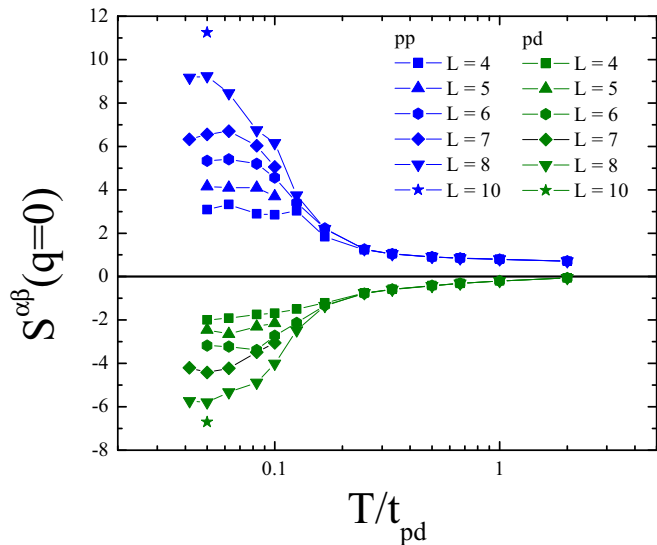
FIG. 4. The FM structure factors $S^{\alpha\beta}(\mathbf{q} = 0,0)$ of the Lieb lattice are plotted as functions of temperature for different lattice sizes L. for $U/t_{pd} = 4$. The relative signs $S^{p^x,p^x}[\mathbf{q} = (0,0)] > 0$ and $S^{d,p^x}[\mathbf{q} = (0,0)] < 0$ are signatures of ferrimagnetism. At high T, where the real space correlations are short range, $S^{\alpha\beta}$ is independent of L. As T decreases, $S^{\alpha\beta}$ plateaus at successively larger values for increasing L, providing evidence that spin correlations extend over the entire lattice.

$T/t_{pd} = 0.042$. Along a path which only includes p sites [(blue) curve going solely through diamond data points], correlations are always positive, indicating a ferromagnetic alignment, and with a robust persistence at large distances. By contrast, along a horizontal path which includes both d and p sites, the correlations alternate in sign, consistently with AFM alignment between d and p sites, and a FM alignment between d sites; here again, the persistence of correlations at large distances ($\sim L/2$) suggests an overall long range FM order. Also shown in Fig. 3(b) are data for the Heisenberg model on the same lattice, which corresponds to the strong coupling limit ($U \gg t_{pd}$) of the Hubbard model; these latter data have been obtained through the stochastic series expansions (SSE) method [39,40]. The amplitudes for $U/t_{pd} = 4$ are still quite far from their strong coupling limit, but one can infer that the slow decay of correlations is a dominant feature, which can therefore being taken as indicative of long range order in the ground state for all U_{pd}.

At high temperatures, $c^{\alpha\beta}(\mathbf{r})$ is short ranged, so the sum over all lattice sites in the structure factor is independent of system size. This is reflected in the high-temperature collapse of $S^{\alpha\beta}[\mathbf{q} = (0,0)]$ in Fig. 4. Data for $S^{\alpha\beta}[\mathbf{q} = (0,0)]$ for different L split apart at $T \sim J$.

A more rigorous probe of long range order is carried out through finite-size scaling analyses [41]. The square of the order parameter is obtained by normalizing the structure factor to the lattice size $m_{\mathbf{q}}^2 = S^{\alpha\beta}(\mathbf{q})/L^2$. This will have a nonzero value in the thermodynamic limit $1/L \to 0$, if $c^{\alpha\beta}(\mathbf{r})$ is long ranged, with a $1/L$ correction. In Fig. 5 data for the global FM structure factor are displayed, for several values of U; also shown are data for the Heisenberg model on the same lattice.
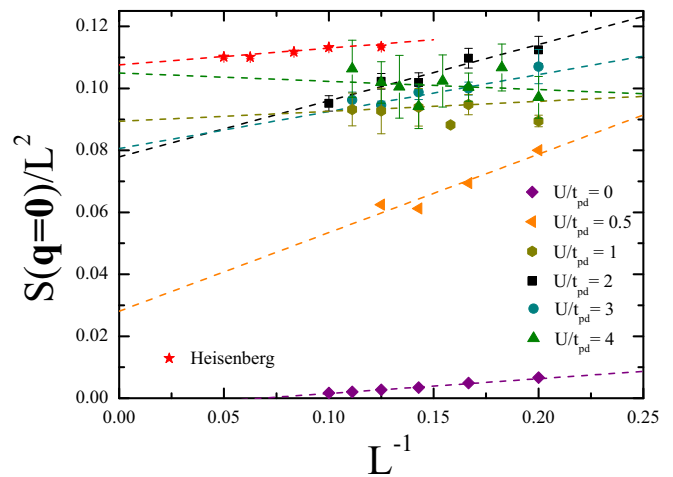

FIG. 5. Finite-size scaling plots for the normalized ground state structure factor m_F^2. For each $U \neq 0$, they extrapolate to a nonzero value in the thermodynamic limit. The data labeled Heisenberg have been obtained for localized spins on Lieb lattice, interacting through nearest-neighbor exchange coupling $\mathbf{S}_i \cdot \mathbf{S}_j$; see text.

The extrapolated values of the order parameter are shown in Fig. 6, as a function of U, thus confirming the existence of long range ferromagnetic order for all $U > 0$. Note that m_F rises sharply for $U/t_{pd} \lesssim 1$, and then stabilizes towards the Heisenberg model value for large U/t_{pd}. At this point, a technical remark is worth making: for $U/t_{pd} \gtrsim 4$ one has to perform simulations at very low temperatures ($T \lesssim 0.025 t_{pd}$, or $\beta \equiv t_{pd}/T = 40$) in order to ensure the structure factor has stabilized; these temperatures are much lower than those needed for the simple square lattice with the same U/t, $\beta \gtrsim 25$ [42].

If we now perform separate finite-size scaling analyses for the structure factors in the different channels $S^{\alpha\beta}(\mathbf{q})$ with
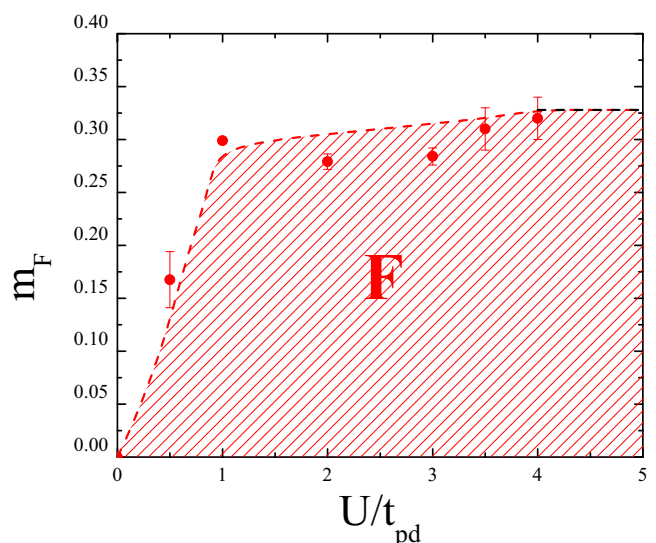

FIG. 6. Global ferromagnetic order parameter as a function of the on-site repulsion U obtained from the extrapolated values, Fig. 5. The (red) dashed line going through the data points is a guide to the eye, while the horizontal (black) dashed line is the Heisenberg limit.
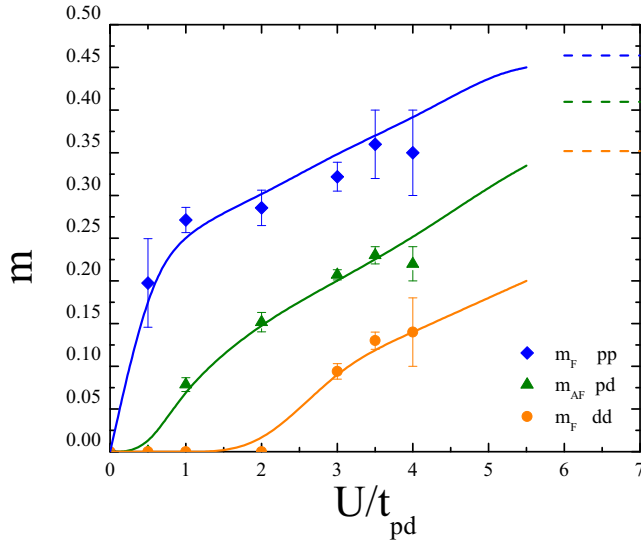
FIG. 7. Extrapolated ($L \to \infty$) values of the channel-resolved order parameters obtained from the scaling of the structure factor; see text. For the FM channels (dd and pp) we set $\mathbf{q} = 0$ in Eq. (4), while for the AFM channel (dp) the sum is carried out with opposite signs at adjacent sites. $\mathbf{q} = (\pi, \pi)$.

$\alpha, \beta = d, p^x, p^y$, we can probe the corresponding sublattice order parameters; their dependence with U is shown in Fig. 7. It is interesting to see that pp ferromagnetism rises sharply with U, in marked contrast to the very slow rise in the dd sublattice. A strong coupling analysis of the $p^y dp^x$ cluster of three Heisenberg-coupled spins reveals that the two p spins form a triplet, which adds to the d spin, leading to a total spin $S_{cluster} = 1/2$ characterizing a *ferrimagnetic* state; this picture can also be applied in weak coupling, as a result of the flat p band. We may therefore attribute the sharper rise of the pp FM order parameter as due to the p spins locking into triplets as soon as U is switched on, while the d spin is somewhat shielded by the surrounding triplets. Figure 7 also shows that the data converge very slowly to the Heisenberg limit; again this may be attributed to the difference in the number of nearest neighbors of p and d sites.

It is also worth checking the insulating nature of the ferrimagnetic state. To this end, we calculate the density of states $N(\omega)$ from DQMC data for the imaginary-time dependent Green's function, which is achieved by inverting the integral equation

$$G(\tau) = \int d\omega N(\omega) \frac{e^{-\omega\tau}}{e^{\beta\omega} + 1}. \tag{6}$$

This inversion can be done, for example, with the "maximum entropy" method [43]. In the case of the square lattice, $N(\omega)$ exhibits a gap at half-filling [7]; this "Slater" gap originates in AFM order at weak U and crosses over into a Mott gap at strong coupling.

Figure 8 shows the projected density of states for the Lieb lattice. We see that at sufficiently low temperatures an insulating gap develops for both orbitals, similarly to the square lattice, but with the important difference that in the present case it results from a ferromagnetic state. Furthermore, the density of states on the p sites displays a double-peak
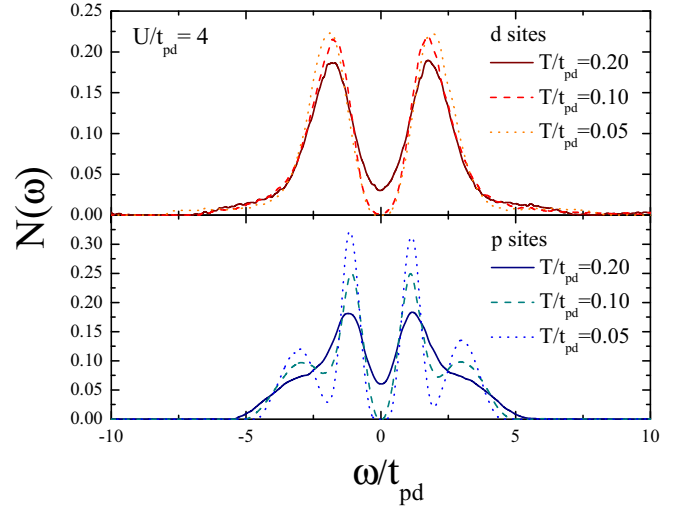

FIG. 8. Local density of states on d sites (top panel) and on p sites (bottom panel), at three different temperatures.

structure on each side of the Fermi energy. The additional peaks originate from the splitting of the flat band on the p sites when a ferromagnetic state is formed; this is similar to what happens in the periodic Anderson model when the Kondo resonance is split when an antiferromagnetic state is formed. We have also obtained the density of states for other values of U. The gap increases monotonically with U.

IV. THE INHOMOGENEOUS LATTICES

The strong coupling limit of a generic inhomogeneous Lieb lattice at half-filling (single occupancy enforced on every site), and with $U_d \neq U_p$, $U_d, U_p > 0$ corresponds to a Heisenberg model with uniform exchange [44]

$$J' = \frac{4t^2}{\widetilde{U}}, \tag{7}$$

where $\widetilde{U}$ is the geometric mean between the on-site repulsion on adjacent sites,

$$\widetilde{U} = \frac{2U_p U_d}{U_p + U_d}. \tag{8}$$

Since one of the steps in Lieb's proof relies on the strong coupling limit of the Hubbard model [22,45], the existence of a ferromagnetic state also holds in this case. This is discussed further in the conclusions.

However, if either U_d or U_p vanishes, this correspondence with the Heisenberg model completely breaks down—single occupancy on every site is no longer guaranteed even at half-filling. Furthermore, due to the different neighborhoods of the d sites (four p neighbors) and of the p sites (two d neighbors), switching off U_d or U_p leads to radically different effects, as we now discuss. Figure 9 displays data for the compressibility. We see that when $U_d = 0$ the system behaves as an insulator; by contrast, when $U_p = 0$ the compressibility increases as the temperature decreases, indicating a metallic state. Therefore, when $U_d = 0$ and at half-filling, each p site is occupied by one fermion, so that the d site is also singly occupied, as if U_d were nonzero; from the magnetic point of view, one then expects a
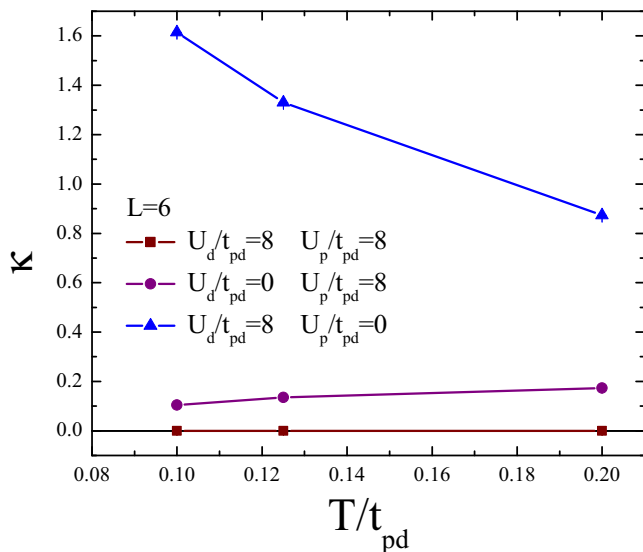
FIG. 9. Comparison of the compressibility at half-filling in three instances: homogeneous lattice (squares), $U_d = 0$ (circles), and $U_p = 0$ (triangles). When nonzero, the Us are all set to $8t_{pd}$; the linear lattice size is $L = 6$.

FIG. 11. Spin correlations between first neighborlike sites. The upper panel displays the correlations between d sites, while the lower panel shows those between p sites; in the latter case, the p sites may have an intervening d site (filled symbols), or not (empty symbols). Data for the usual square lattice are shown, but the fair comparison in this case is with sites on different sublattices (hence two lattice spacings apart, or $r = 2$); see text.

ferromagnetic ground state, just as in the homogeneous case. When $U_p = 0$ the likelihood of double occupancy of the p sites increases, thus destroying any magnetic ordering. As we will see, these expectations are borne out by our simulations.

Figure 10 compares the local moment in the homogeneous and inhomogeneous Lieb lattices. One immediate effect of switching off the repulsion on a subset of sites is the strong suppression of the local moment on exactly those "free" sites; this suppression is almost complete (becoming very near the minimum value of 1/2) on p sites when $U_p = 0$. However, when $U_d = 0$ and $U_p \lesssim 4t_{pd}$ the local moment on the p sites is
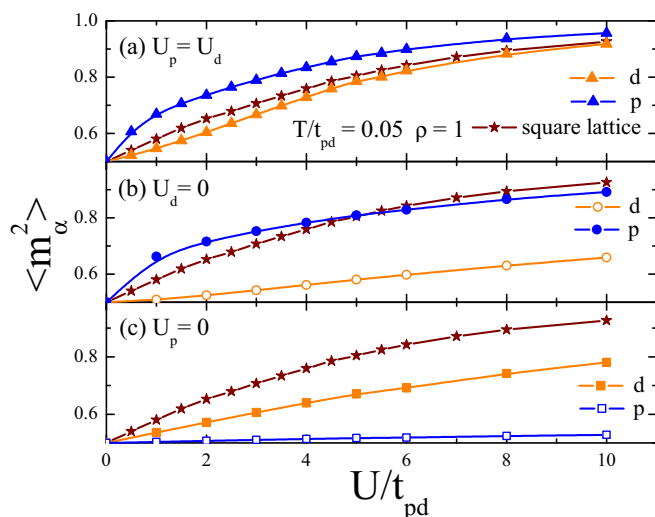

FIG. 10. Local moment on d sites [light (orange) color] and on p sites [dark (blue) color], as functions of the on-site repulsion for (a) the homogeneous case, (b) $U_p = U$, $U_d = 0$, and (c) $U_d = U$, $U_p = 0$. Data for the usual square lattice are also shown (stars), for comparison.
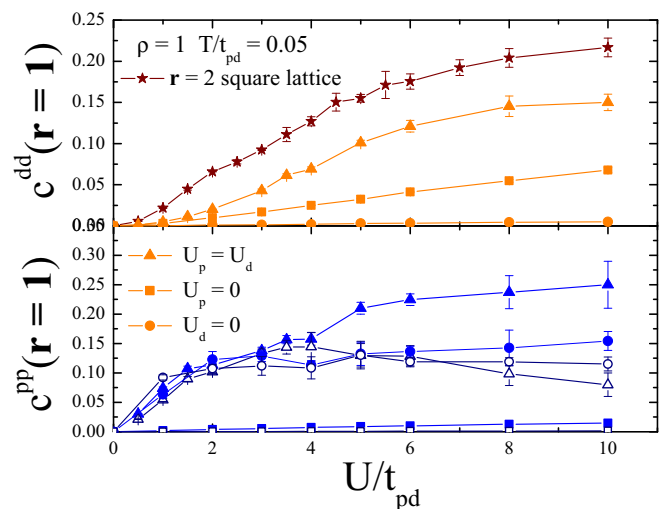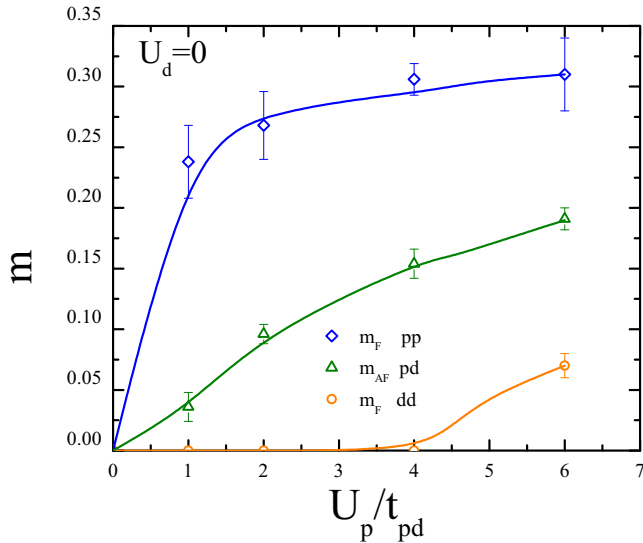
not significantly affected in comparison with the homogeneous case; for $U \gtrsim 4t_{pd}$ it becomes slightly smaller than the one for the square lattice. By contrast, when $U_p = 0$ the suppression of $\langle m^2 \rangle$ on the d sites takes place for all U, as a result of increasing double occupancy.
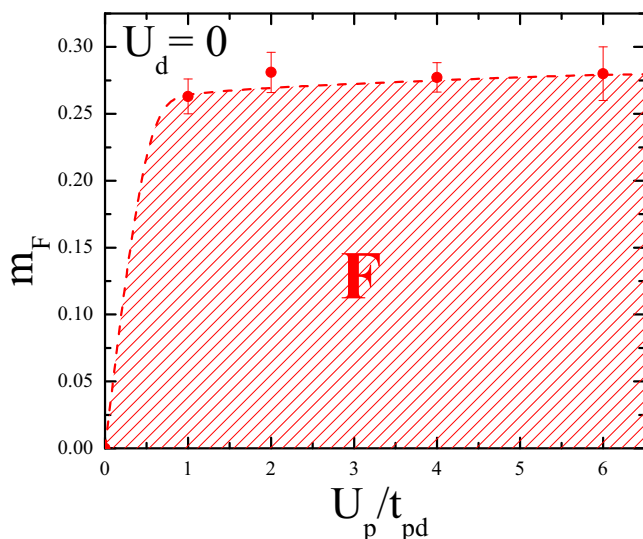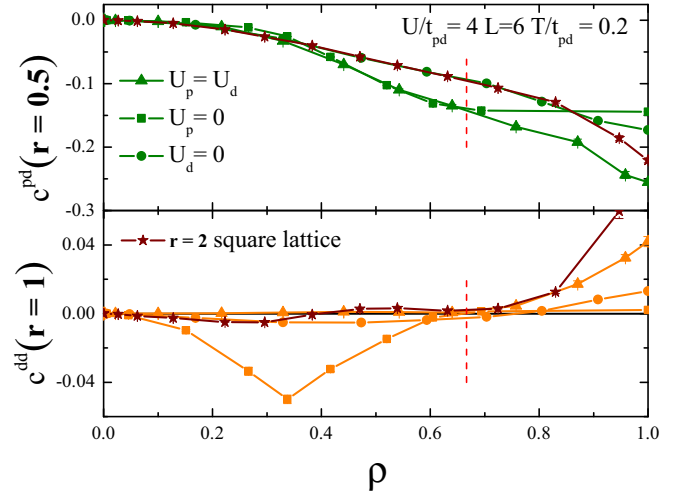
In Fig. 11 we show the spin correlation between sites one lattice spacing apart, as functions of the on-site repulsion. The dd correlations for the homogeneous Lieb lattice are suppressed in comparison with those for the square lattice. As noted earlier in connection with Fig. 2, the local moment on the d site is smaller than on the square lattice, so this reduction in correlations between spins on d sites is expected. For the inhomogeneous Lieb lattice, correlations between spins on d sites are suppressed even more, with those on the d sites being completely suppressed when $U_d = 0$. By contrast, the pp correlations are quite robust if the Coulomb repulsion is only switched off on the d sites; when $U_p = 0$, pp correlations are strongly suppressed. As anticipated, repulsion on the p sites is crucial to the onset of ferromagnetic correlations. At this point, a comment should be made: in the strong coupling (i.e., Heisenberg) limit, pp correlations one lattice spacing apart are exactly the same irrespective of including, or not, an intervening d site. However, up to the couplings covered in Fig. 11, the noticeable difference is due to both the temperature not being low enough, and to the coupling being not so strong.

This is even more evident when we probe long range order (LRO) through finite-size scaling analyses of the $m_{\alpha,\beta}^2 = S^{\alpha,\beta}/L^2$. When $U_p = 0$ the overall ferromagnetic order parameter decreases very fast as $L \to \infty$, indicating the absence of LRO. This is reminiscent of what happens in the diluted Hubbard model on a square lattice. LRO in the ground state is only possible below a certain threshold f_c of free sites, which depends on the strength of the on-site interaction [46–48]: here an effective fraction of free sites can be taken as $f = 2/3$,

FIG. 12. Same as Fig. 7, but now for the $U_d = 0$ case.

FIG. 14. Spin correlation functions as functions of band filling at fixed temperature $T = 0.17t_{pd}$, for a lattice with 6×6 ppd cells, highlighting the differences between homogeneous and both inhomogeneous cases. Top panel: Correlations between spins on nearest s and p sites. Bottom panel: Correlations between spins on nearest d sites.

which is above the thresholds $f_c^{\text{square}}(U = 8t) \simeq 0.4$, and for $f_c^{\text{square}}(U = -4t) \simeq 0.3$. This is consistent with previous work on the case $U_p = 0$ in models of CuO_2 sheets of cuprate superconductors, which do not display an antiferromagnetic ground state, unless a site energy difference $\varepsilon_p - \varepsilon_d > 0$ is included to enhance charge disproportionation [49,50].

For $U_d = 0$, a finite-size scaling analysis of the overall ferromagnetic order parameter indicates LRO. The channel-resolved extrapolated order parameters shown in Fig. 12 are very similar to those for the homogeneous case; the same is true for the global ferromagnetic order parameter, as shown in Fig. 13. We therefore conclude that the preconditions for ferromagnetism on Lieb lattices, at least as far as homogeneity

is concerned, are less restrictive than those originally assumed in Lieb's proof of the theorem.

V. AWAY FROM HALF-FILLING

Away from half-filling, the "minus-sign problem" (see, e.g., Refs. [38,51]) hinders a thorough analysis at low temperatures. Nonetheless, some interesting conclusions may be drawn at accessible temperatures (down to $T/t_{pd} = 0.17$, or $T/W = 0.03$ in units of the noninteracting bandwidth $W = 4\sqrt{2}t$). Figure 14 (top) shows that correlations between spins on near neighbor p and d sites, $c^{pd}(r = 0.5)$, are always AF (negative) and increase monotonically in magnitude with ρ, up to half-filling $\rho = 1$, in both the H and IH cases. The correlations between pairs of d sites, $c^{dd}(r = 1)$, Fig. 14 (bottom), show a more intriguing behavior. $c^{dd}(r = 1)$ is small except near half-filling where it turns relatively strongly positive for the H case (though less large than on a square lattice), and weakly positive for the IH case with $U_d = 0$.

The richest structure is exhibited by $c^{dd}(r = 1)$ for the IH case with $U_p = 0$. It is largest in absolute value at filling $\rho = 1/3$, one fermion on each d site, while the p sites are left empty. This corresponds rather closely to the situation of the CuO_2 planes in cuprates where $U_d > U_p$ and the parent compound La_2CuO_4 has one hole per copper atom. In the cuprates, the site hole energy difference $\varepsilon_p - \varepsilon_d$ is substantial, confining the holes to the copper sites, which would enhance AF order further. The important message of Fig. 14 (bottom) is that even in the absence of a substantial $\varepsilon_p - \varepsilon_d$ there is robust (local) AF order.

FIG. 13. Global ferromagnetic order parameter as a function of the on-site repulsion U_p/t_{pd} obtained from the extrapolated values for the case $U_d = 0$. The (red) dashed line going through the data points is a guide to the eye.

VI. CONCLUSIONS

As with the Anderson localization problem, where two dimensions occupies a special position, itinerant ferromagnetism in 2D lies poised between the 1D case where it is explicitly

forbidden [45] and 3D where it is (fairly) commonly observed in nature; bounds on correlation functions for the Hubbard model (and some variants) in one and two dimensions rule out any magnetic ordering at finite temperatures [52]. One route to ferromagnetism was devised by Lieb [22], who proved that the half-filled Hubbard model on a bipartite lattice with unequal number of sites on each sublattice has a nonzero total spin. A particular geometry to which this applies is the "decorated square lattice," also known as CuO_2 lattice, or Lieb lattice: d sites on the vertices of a square lattice have p sites as nearest neighbors at the midpoints between the d sites; see Fig. 1. In this paper we have used quantum Monte Carlo to unveil several details about the Lieb lattice, by considering both the homogeneous case (on-site repulsion U has the same magnitude on every site), as well as inhomogeneous cases, switching off U on either p or d sites.

For the homogeneous case, we have established that the magnitude of the local moment is strongly dependent on the environment, being larger on the p sites than on the d sites: fewer neighbors leads to a decrease in itinerancy. By analyzing the spatial decay of spin correlation functions, and the lattice-size dependence of magnetic structure factor, we have also provided numerical evidence for the existence of long range ferromagnetic (or *ferrimagnetic*) order. Interestingly, the breakup into sublattice order parameters reveals that the ferromagnetism of spins on p sites is the most intense in magnitude, followed by the antiferromagnetism along the square lattice directions ($d-p$ sites), with the ferromagnetism of d sites being the weakest. These combine to yield an overall ferromagnetic order parameter displaying a sharp rise in the region $U/t_{pd} \lesssim 1$, and stabilizing towards the Heisenberg limit for $U/t_{pd} \gg 1$. Furthermore, by examining the projected density of states (obtained with the aid of the maximum entropy method), we see that the system is an insulator, which is confirmed by compressibility data.

In Lieb's original proof, the on-site repulsion was assumed to be uniform in order to satisfy particle-hole symmetry. However, with the manifestly symmetric form of the Hubbard Hamiltonian considered here, this restriction is removed, and the system is particle-hole symmetric at half-filling for any distribution of U_i through the lattice sites **i**. Furthermore, the strong coupling limit needed to extend the proof to the inhomogeneous lattice is provided by a subsequent work [44], which established that when two adjacent sites had different values of U, say $U_p \neq U_d$, the exchange coupling becomes

$4t^2/\widetilde{U}$, with $\widetilde{U}$ being the geometric mean between U_p and U_d, provided single occupancy could be enforced in this limit. Therefore, ferromagnetism is also expected to occur when $U_p \neq U_d > 0$.

However, this strong coupling limit breaks down when either U_p or U_d vanishes so we have also examined this situation. From our QMC simulations we established that switching off U_d preserves the ferromagnetic state with the same main features of the homogeneous case, while switching off U_p suppresses ferromagnetism (or any other magnetically ordered state). Once again, the different environments of the sites with nonzero repulsion is responsible for this: when $U_p = 0$ the system is metallic, and single occupancy of the p sites is no longer guaranteed.

We have also considered doping away from half-filling. An interesting feature develops in the dd spin correlations when $U_p = 0$ strong antiferromagnetic correlations; they attain a large negative value at $\rho = 1/3$, caused by occupancy of each d site by a single fermion. Previous studies [49] examined the occupations, local moments, and pairing for a range of $\epsilon_p - \epsilon_d$, including $\epsilon_p - \epsilon_d = 0$, but the sharp feature in the dd spin correlations in this case was not noted.

In closing, we should mention that the quantitative exploration of itinerant ferromagnetism remains a key area of strongly correlated electron systems. Recently, ferromagnetism has also been observed in the absence of a lattice in mixtures of ^6Li atoms in two hyperfine states [53]. Lattice models remain more challenging for such optical lattice emulation, owing to the difficulty in cooling the atoms below the ordering temperature, and because of the density inhomogeneity introduced by the confining potential. Progress in observing antiferromagnetism in the single band Hubbard model in one [54], two [55,56], and three [57] dimensions is ongoing. Because of the tunability of these cold atom systems, and particularly the fact that different geometries and regimes of very large U can be accessed, it is possible that new insight into Hubbard model ferromagnetism is on the horizon.

[1] J. Hubbard, Proc. R. Soc. London Ser. A **276**, 238 (1963).

[2] J. E. Hirsch, Phys. Rev. B **31**, 4403 (1985).

[3] P. Fazekas, *Lecture Notes on Electron Correlation and Magnetism*, Series in Modern Condensed Matter Physics (World Scientific, Singapore, 1999).

[4] V. Bach, E. H. Lieb, and J. P. Solovej, J. Stat. Phys. **76**, 3 (1994).

[5] V. Bach and J. Poelchau, J. Math. Phys. **38**, 2072 (1997).

[6] J. E. Hirsch and S. Tang, Phys. Rev. Lett. **62**, 591 (1989).

[7] S. R. White, D. J. Scalapino, R. L. Sugar, E. Y. Loh, J. E. Gubernatis, and R. T. Scalettar, Phys. Rev. B **40**, 506 (1989).

[8] S. Rudin and D. C. Mattis, Phys. Lett. A **110**, 273 (1985).

[9] T. Hanisch and E. Muller-Hartmann, Ann. Phys. **505**, 381 (1993).

[10] F. H. Zong, C. Lin, and D. M. Ceperley, Phys. Rev. E **66**, 036703 (2002).

[11] E. C. Stoner, Proc. R. Soc. London Ser. A **165**, 372 (1938).

[12] A. Mielke, J. Phys. A: Math. Gen. **24**, L73 (1991).

[13] M. Ulmke, Eur. Phys. J. B **1**, 301 (1998).

[14] D. Vollhardt, N. Blümer, K. Held, and M. Kollar, in *Band-Ferromagnetism: Ground-State and Finite-Temperature Phenomena* (Springer, Berlin, 2001), pp. 191–207.

[15] J. E. Hirsch, Phys. Rev. B **40**, 2354 (1989).

[16] R. Strack and D. Vollhardt, Phys. Rev. Lett. **72**, 3425 (1994).

[17] J. Wahle, N. Blümer, J. Schlipf, K. Held, and D. Vollhardt, Phys. Rev. B **58**, 12749 (1998).

[18] J. C. Amadon and J. E. Hirsch, Phys. Rev. B **54**, 6364 (1996).

[19] M. Kollar and D. Vollhardt, Phys. Rev. B **63**, 045107 (2001).

[20] K. Held and D. Vollhardt, Eur. Phys. J. B **5**, 473 (1998).

[21] A. Mielke, Phys. Lett. A **174**, 443 (1993).

[22] E. H. Lieb, Phys. Rev. Lett. **62**, 1201 (1989); **62**, 1927 (1989).

[23] S.-Q. Shen, Z.-M. Qiu, and G.-S. Tian, Phys. Rev. Lett. **72**, 1280 (1994).

[24] H. Tasaki, Prog. Theor. Phys. **99**, 489 (1998).

[25] H. Tasaki, J. Phys.: Condens. Matter **10**, 4353 (1998).

[26] H. Tasaki, Phys. Rev. Lett. **69**, 1608 (1992).

[27] A. Mielke, Phys. Rev. Lett. **82**, 4312 (1999).

[28] A. Mielke, J. Phys. A: Math. Gen. **32**, 8411 (1999).

[29] H. Tasaki, Phys. Rev. Lett. **75**, 4678 (1995).

[30] C. Weeks and M. Franz, Phys. Rev. B **82**, 085310 (2010).

[31] A. Zhao and S.-Q. Shen, Phys. Rev. B **85**, 085209 (2012).

[32] M. Niţă, B. Ostahie, and A. Aldea, Phys. Rev. B **87**, 125428 (2013).

[33] K. Noda, A. Koga, N. Kawakami, and T. Pruschke, Phys. Rev. A **80**, 063622 (2009).

[34] K. Noda, K. Inaba, and M. Yamashita, Phys. Rev. A **90**, 043624 (2014).

[35] R. A. Vicencio, C. Cantillano, L. Morales-Inostroza, B. Real, C. Mejía-Cortés, S. Weimann, A. Szameit, and M. I. Molina, Phys. Rev. Lett. **114**, 245503 (2015).

[36] S. Mukherjee, A. Spracklen, D. Choudhury, N. Goldman, P. Öhberg, E. Andersson, and R. R. Thomson, Phys. Rev. Lett. **114**, 245504 (2015).

[37] R. Blankenbecler, D. J. Scalapino, and R. L. Sugar, Phys. Rev. D **24**, 2278 (1981).

[38] R. R. dos Santos, Braz. J. Phys. **33**, 36 (2003).

[39] O. F. Syljuåsen and A. W. Sandvik, Phys. Rev. E **66**, 046701 (2002).

[40] A. W. Sandvik and O. F. Syljuåsen, AIP Conf. Proc. **690**, 299 (2003).

[41] D. A. Huse, Phys. Rev. B **37**, 2380 (1988).

[42] C. N. Varney, C.-R. Lee, Z. J. Bai, S. Chiesa, M. Jarrell, and R. T. Scalettar, Phys. Rev. B **80**, 075116 (2009).

[43] M. Jarrell and J. Gubernatis, Phys. Rep. **269**, 133 (1996).

[44] V. V. França and K. Capelle, Phys. Rev. B **82**, 134405 (2010).

[45] E. Lieb and D. Mattis, Phys. Rev. **125**, 164 (1962).

[46] M. Ulmke, P. J. H. Denteneer, R. T. Scalettar, and G. T. Zimanyi, Europhys. Lett. **42**, 655 (1998).

[47] D. Hurt, E. Odabashian, W. E. Pickett, R. T. Scalettar, F. Mondaini, T. Paiva, and R. R. dos Santos, Phys. Rev. B **72**, 144513 (2005).

[48] F. Mondaini, T. Paiva, R. R. dos Santos, and R. T. Scalettar, Phys. Rev. B **78**, 174519 (2008).

[49] R. T. Scalettar, D. J. Scalapino, R. L. Sugar, and S. R. White, Phys. Rev. B **44**, 770 (1991).

[50] Y. F. Kung, C.-C. Chen, Y. Wang, E. W. Huang, E. A. Nowadnick, B. Moritz, R. T. Scalettar, S. Johnston, and T. P. Devereaux, Phys. Rev. B **93**, 155166 (2016).

[51] E. Y. Loh, J. E. Gubernatis, R. T. Scalettar, S. R. White, D. J. Scalapino, and R. L. Sugar, Phys. Rev. B **41**, 9301 (1990).

[52] T. Koma and H. Tasaki, Phys. Rev. Lett. **68**, 3248 (1992).

[53] G.-B. Jo, Y.-R. Lee, J.-H. Choi, C. A. Christensen, T. H. Kim, J. H. Thywissen, D. E. Pritchard, and W. Ketterle, Science **325**, 1521 (2009).

[54] M. Boll, T. A. Hilker, G. Salomon, A. Omran, J. Nespolo, L. Pollet, I. Bloch, and C. Gross, Science **353**, 1257 (2016).

[55] M. F. Parsons, A. Mazurenko, C. S. Chiu, G. Ji, D. Greif, and M. Greiner, Science **353**, 1253 (2016).

[56] L. W. Cheuk, M. A. Nichols, K. R. Lawrence, M. Okan, H. Zhang, E. Khatami, N. Trivedi, T. Paiva, M. Rigol, and M. W. Zwierlein, Science **353**, 1260 (2016).

[57] R. A. Hart, P. M. Duarte, T.-L. Yang, X. Liu, T. Paiva, E. Khatami, R. T. Scalettar, N. Trivedi, D. A. Huse, and R. G. Hulet, Nature (London) **519**, 211 (2015).